Journal of Sound and Vibration (2001) **247**(4), 741–753
doi:10.1006/jsvi.2001.3664, available online at http://www.idealibrary.com on IDEAL®

A VARIABLE STRUCTURE CONTROL TOGGLE MECHANISM DRIVEN BY A LINEAR SYNCHRONOUS MOTOR WITH JOINT COULOMB FRICTION

R.-F. FUNG

Department of Mechanical and Automation Engineering, National Kaohsiung first University of Science and Technology, University Road, Yuanchau, Kaohsiung 824, *Taiwan, Republic of China. E-mail: rffung@ccms.nkfust.edu.tw*

J.-W. WU

Department of Mechanical Engineering, Chung Yuan Christian University, Chung-Li 32023, *Taiwan, Republic of China.*

AND

D.-S. CHEN

Software and Calibration Tools Department, Powertrain Control Systems Engineering, Ford Motor Company, Dearborn, MI 48121, *U.S.A.*

(*Received* 1 *March* 2001, *and in final form* 28 *March* 2001)

1. INTRODUCTION

The linear synchronous motor (LSM) consists of a primary (or stator) and a secondary (or rotor). The primary contains a three-phase armature winding which is located in the slots of a laminated stationary iron core and is supplied with an armature frequency producing the travelling current density wave of a pole pitch along the track at synchronous speeds. The secondary is composed of a permanent magnet (PM) with a linear array of poles and DC excitation coils. The section of the stator armature winding uncouples the secondary, and produces leakage flux and extra stator resistance. Although an LSM may have large air gaps and a leakage flux, it is much quieter and more reliable than the rotary counterpart used to produce motion in a straight line. Applications of the LSM do not require any convert gears, wormscrews, or other auxiliary mechanisms.

An application of the track-powered LSM with rare-earth magnet material for automated urban transit vehicles was investigated by Slemon *et al.* [1]. The LSM of the PM type [2] has analytical expressions for the field distributions and this type of model is a single-sided flat PMLSM. Using a dynamic modelling of the controlled-PM LSM, Yoshida and Umino [3] designed a state feedback control for propulsion and levitation systems. The force of an air-core flat PM self-synchronous linear motor was also investigated for an idealized rectangular current inverter control in reference [4]. To determine the electromagnetic force and parameters of a PMLSM, Boldea *et al.* [5] employed the concept of magnetic charge.

Sensitivity and kinematic analyses of a toggle mechanism including the position, velocity, and acceleration were analyzed in reference [6]. The structure of the toggle mechanism is shown in Figure 1. Most applications of the toggle mechanism are in the cases where a large

0022-460X/01/440741 + 13 $35.00/0

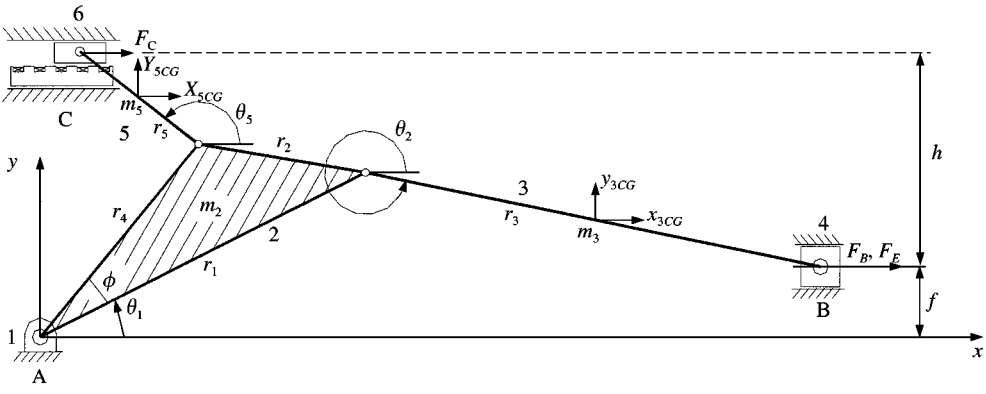

Figure 1. Toggle mechanism driven by a PMLSM.

conducting force is needed with a small driving force acting on a short distance. When the external force F_C generated by an LSM exerted on the slider C, the force is rapidly transmitted to drive the slider B. Since the toggle mechanism has one degree of freedom (d.o.f.), the angles θ_2 and θ_5, and the output position of slider B correspond to one and only one angle θ_1. For a given position, velocity, and acceleration of slider B, the inverse dynamic force acting on each part of the toggle mechanism may be calculated [7]. The position control of the output slider of the toggle mechanism using a PM synchronous servomotor drive via the sliding mode and fuzzy controllers has been reported by Lin *et al.* [8].

Traditional techniques of controlling a rotary motor to drive the toggle mechanism have been presented in the previous studies [6–8]. But they have some shortcomings such as increasing losses of the transmission efficiency, frictional forces, and noises between connections. To date, it appears that no study has investigated the toggle mechanism driven by a PMLSM drive, and the effect of Coulomb friction on the toggle mechanism was not considered in the dynamic analysis. Traditional methods of solving the problem of Coulomb friction are based on friction circles, and it is difficult to handle equilibrium equations of the non-linear terms. Wang *et al.* [9] developed an approach for the dynamic simulation of mechanical systems with multiple frictional contacts. Dupont and Yamajako [10] obtained the stability of frictional contacts in the constrained rigid-body dynamics.

This paper presents a new application of the toggle mechanism driven by a controlled-PM LSM as shown in Figure 1. Using the proposed LSM as a replacement of gears and other auxiliary mechanisms, we have the benefits of reduced frictions, reliability, and quietness. In the propulsion system, the exciting currents in the stator windings along the guideway are controlled to obtain the required dynamic performance for the toggle mechanism drive. Finally, numerical results for driving forces and controlled responses with and without Coulomb friction in the joints between the given stroke of slider B are presented.

2. DYNAMIC ANALYSIS

2.1. THRUST ANALYSIS

A general model [11] of a flat, single-sided, permanent magnet linear synchronous motor (PMLSM) is shown in Figure 2. The flat configuration divides the system into two regions.

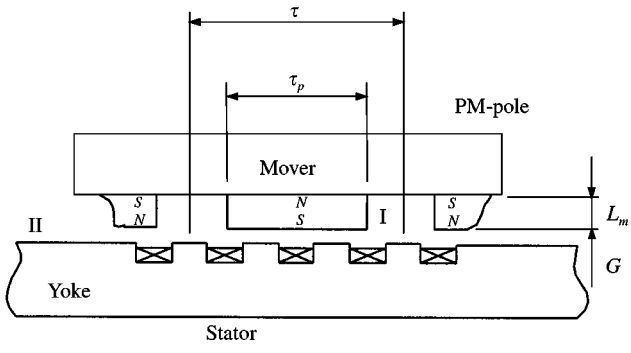

Figure 2. The PMLSM with a short PM-pole mover.

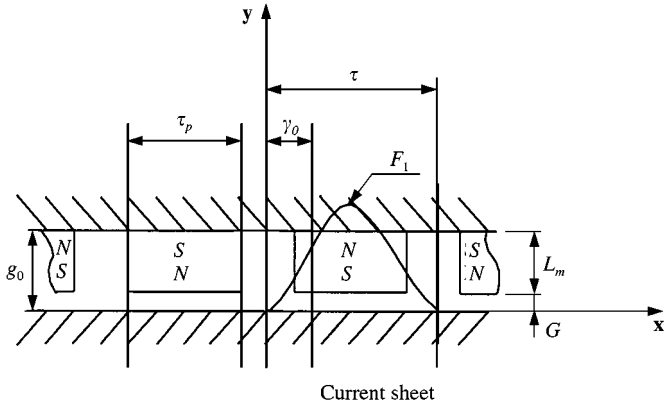

Figure 3. System model of region I.

Region I is the air gap between the stator and mover and region II represents the open air gap above the stator.

The model of the PMLSM for mathematical analysis is given in Figure 3. In essence, the slotted primary structure with its winding is not an ideal boundary where the solutions to the governing field equations cannot be obtained. To overcome this problem, the actual slotted structure may be replaced by a smooth surface and the current-carrying windings may be regarded as infinitely fictitious thin current elements called current sheets, which have linear current density. Thus, the actual air gap of the PMLSM may be replaced by an effective air gap. Here, the governing equation with respect to the scalar potential $\psi_{m\mathrm{I}}$ for the region I is denoted as

$$\nabla^2 \psi_{m\mathrm{I}} = 0. \tag{1}$$

The boundary conditions are as follows:

$$\psi_{m\mathrm{I}} = 0 \quad \text{at } y = g_0, \qquad \psi_{m\mathrm{I}} = F_1 \sin \frac{\pi}{\tau} x \quad \text{at } y = 0, \tag{2, 3}$$

in which

$$g_0 = L_m + G, \quad F_1 = \frac{6\sqrt{2}}{K_C \pi} \left(\frac{K_{W1} W}{p} \right) I,$$

where τ is the pole pitch, L_m the height of the PM poles, G the length of the air gap between the PM poles and the stator, F_1 the fundamental component of the MMF (magnetomotive force), K_C stands for Carter's coefficient which replaces the slot structure of the stator by an effective air gap, K_{W1} the total winding factor, W the series turns per phase, p the number of poles of the stator winding, and I refers to the armature phase current.

Solving equation (1) with the given conditions (2) and (3), one obtains

$$\psi_{m\mathrm{I}} = F_1 \left(\cosh \frac{\pi}{\tau} y - k \sinh \frac{\pi}{\tau} y \right) \sin \frac{\pi}{\tau} x, \tag{4}$$

where

$$k = \coth \frac{\pi}{\tau} g_0.$$

Since a magnetostatic field H may be derived from the gradient of a scalar potential ψ_m for the absence of current [4], one can write

$$H = - \nabla \psi_m. \tag{5}$$

The flux density of the air gap in the PMLSM is further given by

$$B = \mu_0 H, \tag{6}$$

where μ_0 is called simply permeability. Substituting equation (5) into equation (6) yields

$$B_{x\mathrm{I}} = \mu_0 H_{x\mathrm{I}} = - \mu_0 \frac{\partial \psi_{mI}}{\partial x}, \tag{7}$$

$$B_{y\mathrm{I}} = \mu_0 H_{y\mathrm{I}} = - \mu_0 \frac{\partial \psi_{mI}}{\partial y}. \tag{8}$$

From equations (4), (7) and (8), one obtains

$$B_{x\mathrm{I}} = - \mu_0 \frac{\pi}{\tau} F_1 \left(\cosh \frac{\pi}{\tau} y - k \sinh \frac{\pi}{\tau} y \right) \cos \left(\frac{\pi}{\tau} x \right), \tag{9}$$

$$B_{y\mathrm{I}} = - \mu_0 \frac{\pi}{\tau} F_1 \left(\sinh \frac{\pi}{\tau} y + k \cosh \frac{\pi}{\tau} y \right) \sin \left(\frac{\pi}{\tau} x \right). \tag{10}$$

In addition, for the magnetic charges (q_m) in a magnetostatic field, the conducting force is described by

$$F = B q_m. \tag{11}$$

The interactive force of these poles with stator travelling on a current density wave by producing a horizontal force from the synchronous travelling magnetic fields is

$$\begin{aligned} F_C &= \sigma_m \iint_s B_x \, \mathrm{d}s \\ &= P_m L_A \sigma_m \int_{-\alpha\tau/2}^{\alpha\tau/2} B_x \sin \left(\frac{\pi}{\tau} x - \gamma_0 \right) \mathrm{d}x, \end{aligned} \tag{12}$$

where P_m is the number of PM poles, L_A the width of poles along the z direction, γ_0 the current load angle, and

$$\alpha = \frac{\tau_p}{\tau} = \frac{\text{pole width of the PM pole}}{\text{pole pitch}}, \tag{13}$$

$$B_x = B_{x1m}|_{y=G}$$

$$= \mu_0 \frac{\pi}{\tau} F_1 \frac{\sinh((\pi/\tau)L_m)}{\sinh((\pi/\tau)(G + L_m))}, \tag{14}$$

$$\sigma_m = \frac{B_r}{\mu_0}, \tag{15}$$

where σ_m stands for the surface density of magnetic charge and B_r is the remanent flux.

Finally, substituting equation (15) into equation (12) yields

$$F_C = \frac{2\tau}{\mu_0 \pi} B_r P_m L_A B_x \sin\frac{\alpha\pi}{2} \sin\gamma_0. \tag{16}$$

2.2. MATHEMATICAL MODEL OF THE COUPLED MECHANISM WITH THE JOINT COULOMB FRICTION

The Hamilton principle and the Lagrange multiplier method are employed to derive the differential–algebraic equation for the toggle mechanism. The detailed derivation could be found in reference [7].

One of the significant factors affecting the dynamic response of the toggle mechanism is the energy dissipating system. The comprehensive studies [9, 10] of sliding joints mechanism have proved the Coulomb friction to be the major source of energy dissipation. The frictional contacts on the joint surfaces serve as the additional forces acting on the system dynamics. The most common approach in treating the geometrical contact problems is based on the Lagrange multiplier method where augmenting the Lagrange multipliers as additional system variables enforces the geometric conditions. According to the joint Coulomb friction concepts developed by Wang *et al.* [9] and Dupont *et al.* [10], the generalized contact friction force in each joint can be expressed as

$$\mathbf{F}_f = \mathbf{Q}_f^T \lambda, \tag{17}$$

where

$$\mathbf{Q}_f^T = \begin{bmatrix} 0 & \mu\,\mathrm{sgn}(\dot{\theta}_5) r_5 \sin\theta_5 \\ -\mu\,\mathrm{sgn}(\dot{\theta}_2) r_3 \sin\theta_2 & 0 \\ -\mu\,\mathrm{sgn}(\dot{\theta}_1) r_1 \sin\theta_1 & \mu\,\mathrm{sgn}(\dot{\theta}_1) r_4 \sin(\theta_1 + \phi) \end{bmatrix}$$

and $\lambda \in \mathbf{R}^{2\times 1}$ is Lagrange multiplier associated with the constraint force, $\mathbf{Q}_f$ is the friction force vector and μ is the coefficient of the dry friction. It can be seen that the generalized constraint friction force is perpendicular to the generalized constraint reaction force. The

sign function of the angular velocities of links 2, 3 and 5 determines whether the generalized normal force is directed along the direction of the constraint surface or not.

Combining equations (17), constraint equation of acceleration, and the governing equation, one obtains an equation in the matrix form

$$\begin{bmatrix} \mathbf{M} & (\mathbf{\Phi}_{\theta}^{\mathrm{T}} + \mathbf{Q}_{f}^{\mathrm{T}}) \\ \mathbf{\Phi}_{\theta} & \mathbf{0} \end{bmatrix} \begin{bmatrix} \ddot{\boldsymbol{\theta}} \\ \boldsymbol{\lambda} \end{bmatrix} = \begin{bmatrix} \mathbf{BU} + \mathbf{D}(\boldsymbol{\theta}) - \mathbf{N}(\boldsymbol{\theta}, \dot{\boldsymbol{\theta}}) \\ \boldsymbol{\gamma} \end{bmatrix}. \tag{18}$$

This is a system of differential–algebraic equations and all the matrix elements are defined in reference [7].

3. TWO-PHASE VSC CONTROLLER DESIGN

Fung *et al.* [12] carried out a two-phase VSC controller scheme on a PM synchronous servomotor and a non-linear electrohydraulic servosystem. The proposed two-phase VSC position controller for the PMLSM toggle mechanism is shown in Figure 5. We adopt the reaching control law [13] and let the switching function to be of the form

$$\dot{S} = -Q\,\mathrm{sgn}(S) - PS, \tag{19}$$

where Q and P are positive constants.

The selection of equation (19) guarantees that the hitting condition

$$S\dot{S} < 0 \tag{20}$$

is satisfied and that the state is confined to the switching surface in finite time. It can be shown that the hitting time [14] of the system (i.e., the time needed for the state trajectory to reach the switching surface) is

$$T_h = \frac{1}{P} \ln\left(\frac{P|S(t_0)|}{Q} + 1\right), \tag{21}$$

where $S(t_0)$ is the initial value of $S(t)$.

Taking the time derivative of the scalar function $S = Ce + \dot{e}$, $C > 0$, yields

$$\dot{S}|_{U_{VSC}=u} = C\dot{e} - f - Gu - d, \tag{22}$$

where u is the two-phase VSC control input function.

Combining equations (19) and (22), the reaching phase controller u_r can be obtained as

$$u_r = G^{-1}(C\dot{e} + PS + Q\,\mathrm{sgn}(S) - f - d). \tag{23}$$

By adding the proportional term, PS, the state is enforced to reach the switching surface faster when S is taken as a large value. In other words, u_r can speed up the state motion toward the switching surface by choosing large values of Q and P, but it may cause the high-frequency chattering phenomenon.

To further improve the system dynamics in the vicinity of the sliding surface $S = 0$, a sliding phase controller [15] is defined as

$$u_s = G^{-1}\left(C\dot{e} + \frac{\beta S}{|S| + \delta} - f - d\right), \tag{24}$$

where $\beta S/(|S| + \delta)$ is a smoothing function which eliminates the chattering phenomenon. The constant β (> 0) may be a large value while δ (> 0) should be chosen as small as possible to avoid the chattering phenomenon.

The two-phase VSC control input $u(t)$ is finally defined as

$$u(t) = ru_r(t) + (1 - r)u_s(t), \tag{25}$$

where

$$r = \begin{cases} 1 & \text{if } t < T_h, \\ 0 & \text{if } t \geqslant T_h. \end{cases}$$

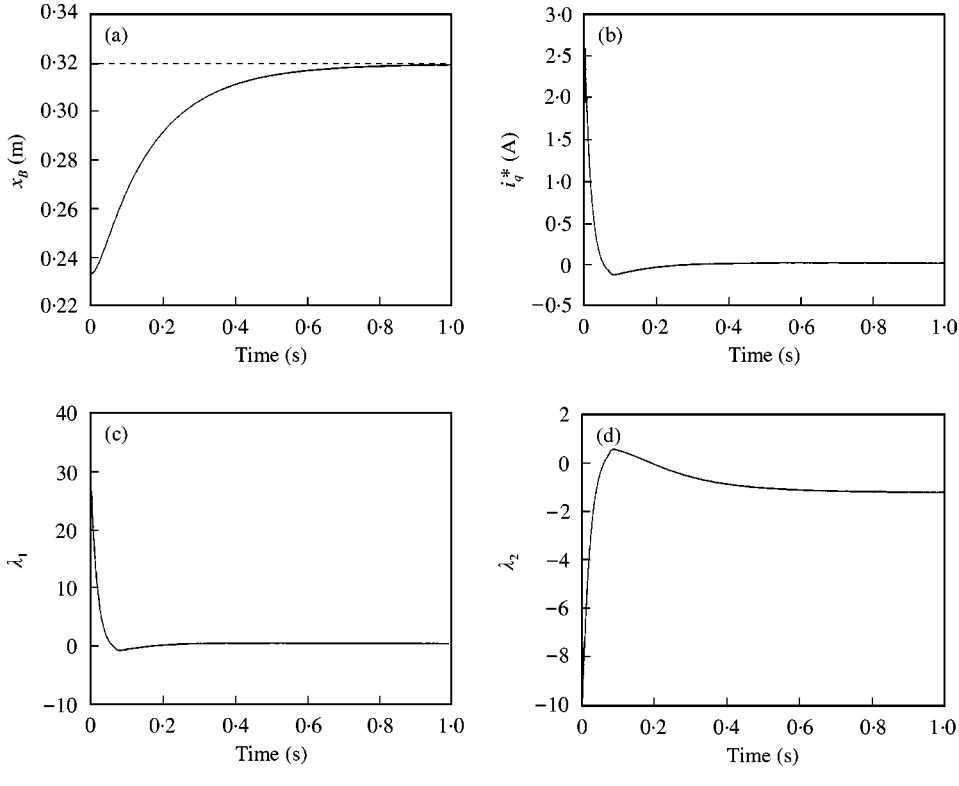

Figure 4. Simulation responses of the two-phase VSC with and without the joint Coulomb friction (nominal case with $F_E = 0$ N): (a) the position of slider B; (b) the control input i_q^*; (c) Lagrange multipliers λ_1: ——, with friction; – · – · –, no friction; (d) Lagrange multipliers λ_2; (e) the contact force at joint (2, 3): ——, normal force; – · – · –, friction force; (f) the contact force at joint (3, 4); (g) the contact force at joint (2, 5); (h) the contact force at joint (5, 6); (i) the contact force at joint (1, 2).

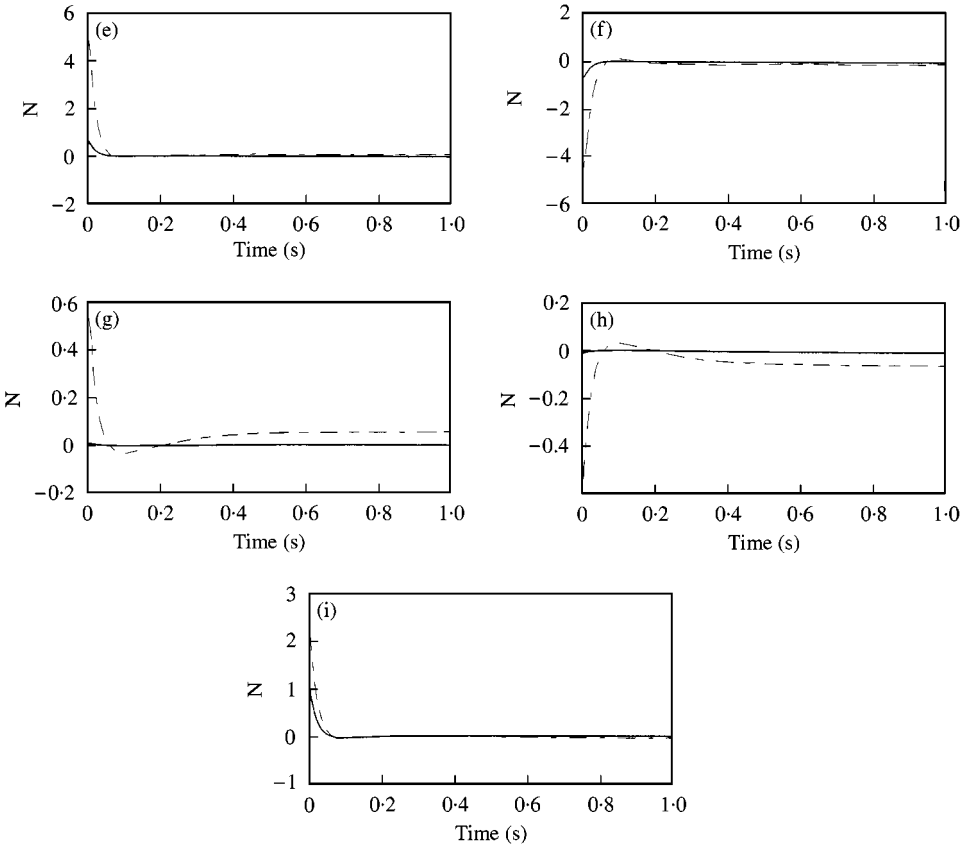

Figure 4. Continued

4. SIMULATION RESULTS AND DISCUSSION

In the following numerical simulations, the parameters of the PMLSM are given by

$$\tau = 0{\cdot}1143 \text{ m}, \quad P_m = 2, \quad B_r = 0{\cdot}86 \text{ T}, \quad L_m = 0{\cdot}00635 \text{ m},$$

$$\alpha = 0{\cdot}67, \quad K_C = 1, \quad G = 0{\cdot}002 \text{ m}, \quad L_A = 0{\cdot}1016 \text{ m},$$

$$K_{WI} = 0{\cdot}955, \quad \gamma_0 = \frac{\pi}{2}, \quad W = 96 \text{ turns}, \quad p = 1.$$

The parameters of the toggle mechanism are chosen as those of reference [8]. The input gains of the control law are selected as follows:

$$C = 5, \quad K = 350, \quad Q = 4,$$

$$P = 50, \quad \delta = 0{\cdot}25, \quad \beta = 65.$$

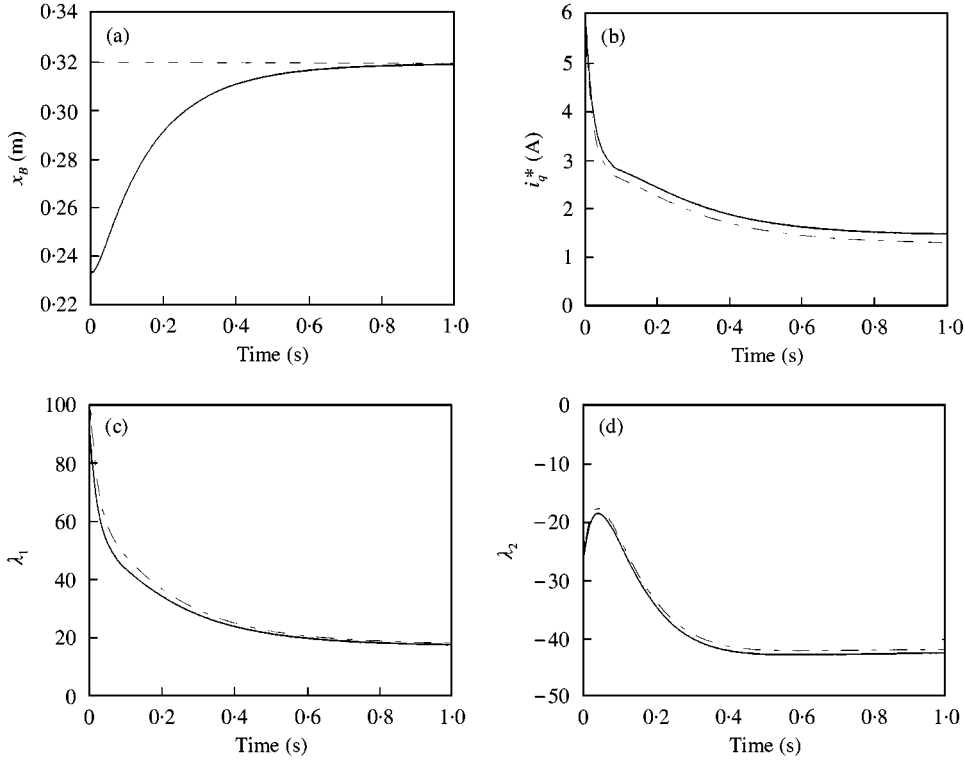

Figure 5. Simulation responses of the two-phase VSC with and without the joint Coulomb friction (nominal case with $F_E = 100$ N): (a) the position of slider B; (b) the control input i_q^*; (c) Lagrange multipliers λ_1: ——, with friction; – · – · –, no friction; (d) Lagrange multipliers λ_2; (e) the contact force at joint (2, 3): ——, normal force; – · – · –, friction force; (f) the contact force at joint (3, 4); (g) the contact force at joint (2, 5); (h) the contact force at joint (5, 6); (i) the contact force at joint (1, 2).

It should be noticed that the input gains listed above are determined for the nominal plant with $F_E = 0$ N. As will be seen, a non-zero external force F_E and a significant plant parameter change in the mass of slider B, m_B, will be introduced for robustness analyses while these input gains remain unchaged. The dry coefficient $\mu = 0{\cdot}2$ is taken as the upper bounded parameter of the Coulomb friction, because the accurate measurement or indentification of Coulomb friction is normally difficult in practice.

In all the simulations, the control objective is to regulate the position of slider B moving from the left to the right end. The initial position of x_B is 0·2329 m, and the desired position x_B^* is 0·3199 m. The effect of Coulomb friction in each joint is considered in the coupled toggle mechanism system by using the Lagrange multiplier method. Substituting x_B and x_B^* into

$$\theta_1 = \sin^{-1}\left[\frac{x_B^2 + r_1^2 + f^2 - r_3^2}{2r_1\sqrt{x_B^2 + f^2}}\right] - \theta_1', \tag{26}$$

where

$$\theta_1' = \sin^{-1}\frac{x_B}{\sqrt{x_B^2 + f^2}},$$

the initial and desired angles θ_1 and θ_1^* can be obtained.

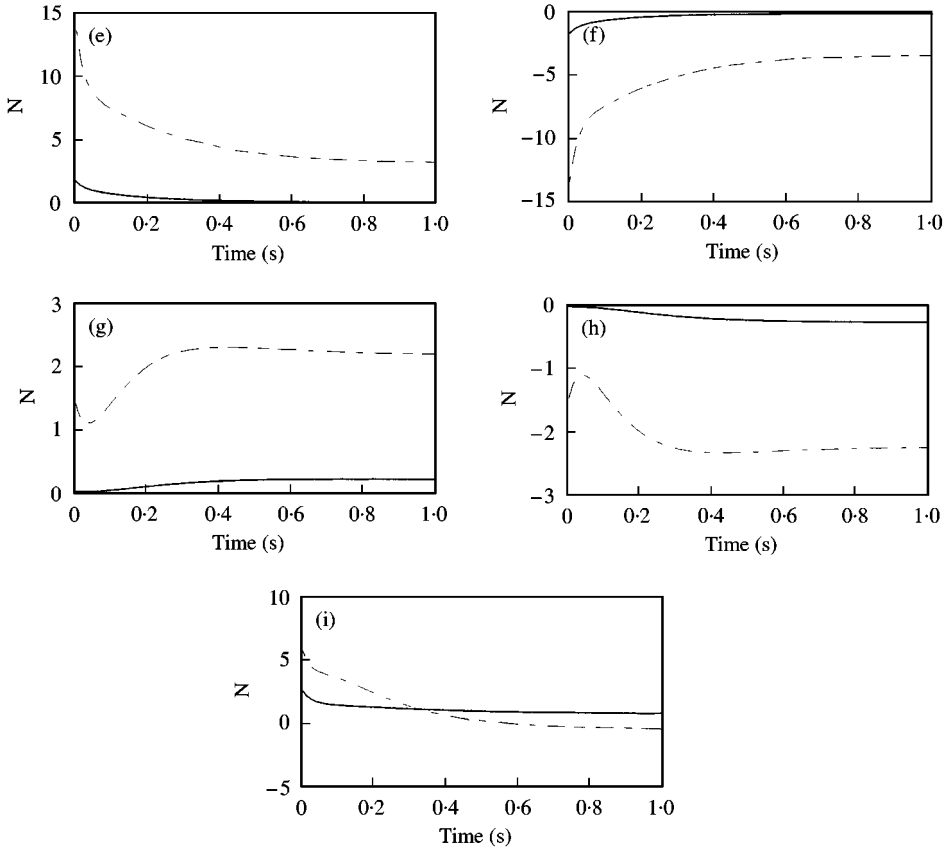

Figure 5. Continued

The simulation results of the nominal case with external disturbance force $F_E = 0$ N are shown in Figure 4(a–i). Then, Figure 5(a–i) illustrates the case with an external disturbance force $F_E = 100$ N. Finally, Figure 6(a–i) demonstrates the simulation results of the parameter variation with an increasing mass o $_B$ to 8·86 kg and an external disturbance force $F_E = 0$ N. Several important results can be observed. (1) For the nominal case, the control inputs i_q^* are almost identical for both cases with and without the joint Coulomb friction. This is because the effect of Coulomb friction is insignificant. (2) While the system is subjected to the external disturbance force, much higher control input i_q^* is needed to drive the mechanism. (3) According to the simulation results, the variable structure controllers are proved to be robust in the presence of external forces and parameter variation.

5. CONCLUSIONS

The Lagrange multiplier method has been applied to the toggle mechanism system with Coulomb friction at each joint. The Lagrange multiplier is a scalar describing the connection of the constraint force and the kinematics constraint. It has been shown that the

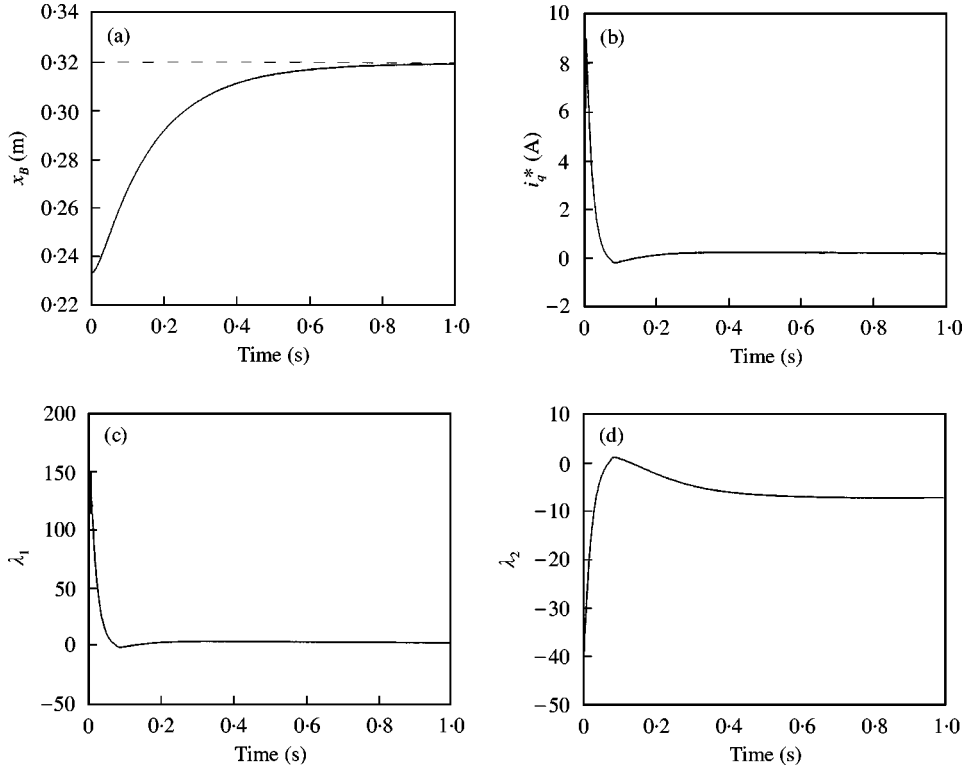

Figure 6. Simulation responses of the two-phase VSC with and without the joint Coulomb friction (parameter variation with $F_E = 0$ N): (a) the position of slider B; (b) the control input i_q^*; (c) Lagrange multipliers λ_1: ——, with friction; – · – · – · –, no friction; (d) Lagrange multipliers λ_2; (e) the contact force at joint (2, 3): ——, normal force; – · – · – · –, friction force; (f) the contact force at joint (3, 4); (g) the contact force at joint (2, 5); (h) the contact force at joint (5, 6); (i) the contact force at joint (1, 2).

friction force is perpendicular to the normal force and is directed along the direction of motion. The position control of the toggle mechanism driven by an LSM using two-phase VSC controller has successfully been studied. Simulation results have revealed that Coulomb friction has the effect of increasing the forces at joints and consuming the energy of the toggle mechanism. It has been observed that more than half of the total input energy was applied to overcome the joint Coulomb friction at the beginning of the system motion.

ACKNOWLEDGMENTS

The authors are greatly inbedted to the National Science Council Republic of China for the support of the research through Contract no. NSC 88-2212-E033-002.

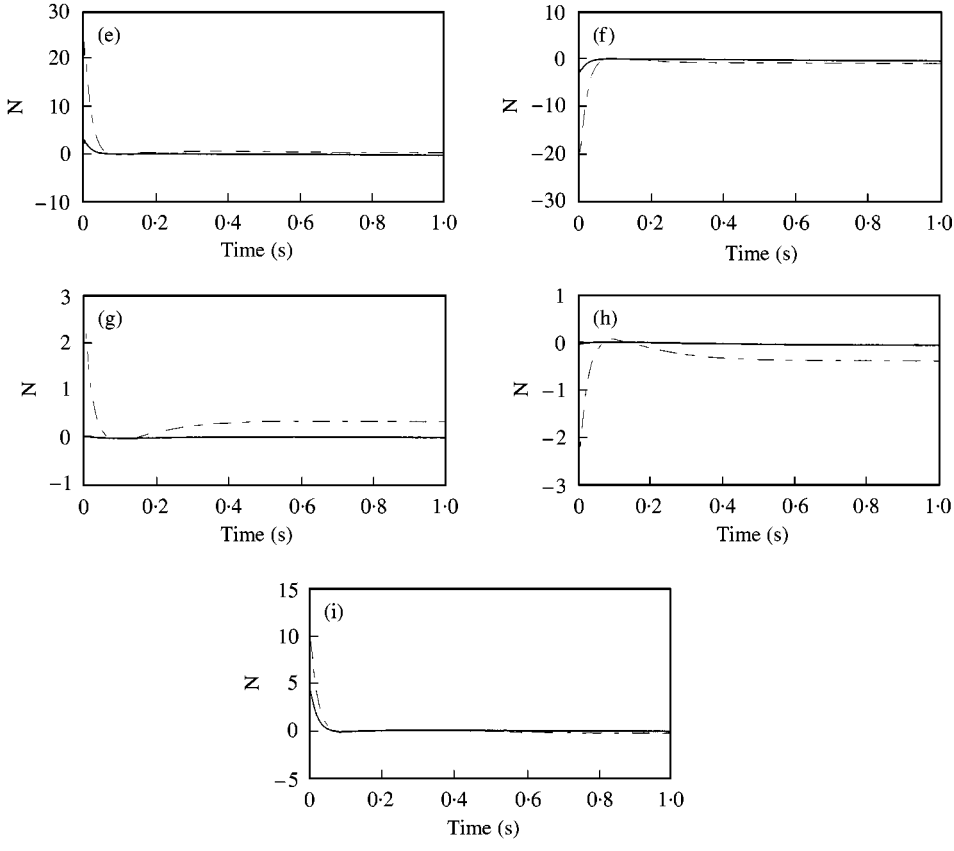

Figure 6. Continued

REFERENCES

1. G. R. SLEMON, P. E. BURKE and N. TERZIS 1978 *IEEE Transactions on Magnetics* **14**, 921–923. A linear synchronous motor for urban transit using rare earth magnets.
2. Z. DENG, I. BOLDEA and S. A. NASAR 1986 *IEEE Transactions on Magnetics* **22**, 107–112. Fields in permanent magnet linear synchronous machines.
3. K. YOSHIDA and T. UMINO 1987 *IEEE Transactions on Magnetics* **23**, 2353–2355. Dynamics of the propulsion and levitation systems in the controlled-PM LSM maglev vehicle.
4. S. A. NASAR and G. Y. XIONG 1988 *IEEE Transactions on Magnetics* **24**, 2038–2044. Determination of field of a permanent-magnet disk machine using the concept of magnetic charge.
5. I. BOLDEA, S. A. NASAR and Z. X. FU 1988 *IEEE Transactions on Magnetics* **24**, 2194–2203. Fields, forces, and performance equations of air-core linear self-synchronous motor with rectangular current control.
6. R. F. FUNG, C. C. HWANG and C. S. HUANG 1997 *The Japan Society of Mechanical Engineers Series C* **40**, 360–365. Kinematic and sensitivity analyses of a new type toggle mechanism.
7. R. F. FUNG, C. C. HUANG, C. S. HUANG and W. P. CHEN 1997 *Computer & Structure* **63**, 91–99. Inverse dynamics of a toggle mechanism.
8. F. J. LIN, R. F. FUNG and Y. C. WANG 1997 *IEEE Proceedings on Control Theory and Applications* **144**, 393–402. Sliding mode and fuzzy control of toggle mechanism using PM synchronous servomotor drive.
9. Y. T. WANG, V. KUMAR, and J. ABEL 1992 *Proceedings of the IEEE International Conference on Robotics and Automation, Nice, France, May*, 2764–2769. Dynamics of rigid bodies undergoing multiple frictional contacts.

10. P. E. DUPONT and P. YAMAJAKO 1997 *IEEE Transactions on Robotics and Automation* **13**, 230–236. Stability of frictional contact in constrained rigid-body dynamics.
11. G. XIONG and S. A. NASAR 1989 *IEEE Transactions on Magnetics* **25**, 2713–2719. Analysis of fields and forces in a permanent magnet linear synchronous machine based on the concept of magnetic charge.
12. R. F. FUNG, F. J. LIN and K. W. CHEN 1996 *International Journal of System Science* **27**, 1265–1273. Application of two-phase VSC with integral compensation in speed control of a PM synchronous servomotor.
13. W. J. WANG and J. L. LEE 1993 *Journal of Control Systems and Technology* **1**, 19–25. Hitting time reduction and chattering attenuation in variable structure systems.
14. R. F. FUNG and C. C. LIAO 1995 *International Journal of Mechanical Science* **37**, 985–993. Application of variable structure control in the nonlinear string system.
15. J. J. E. SLOTINE and W. P. LI 1991 *Applied Nonlinear Control*. Englewood Cliffs, NJ: Prentice-Hall.